

Li-ion電池負極(II)

ハードカーボン系負極

Charge-Discharge Curves of Various Carbon Materials

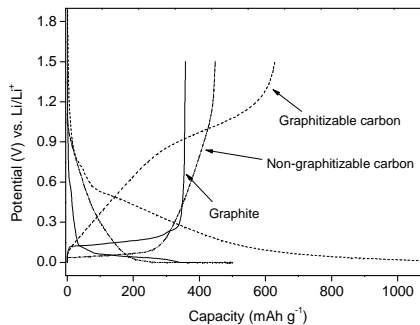


Figure 1-4. Charge-discharge profiles of representative carbon materials

Anodic performance and their related factors

Performances	Factors
Capacity	• Sites for Li incorporation
Potential for charge and discharge	• Reversibility of charge and discharge • Over potential • Non-electrochemical reaction
charge and discharge rate	• Diffusivity of Li
Non-dischargeable charge	• Reactivity of electrolyte • Reactivity of anode, hetero atomic groups, terminal C-H, edge carbon • Irreversible sites for Li incorporation
Cycle ability	• Irreversible charge in structure
Safety	• Stability of charged Li • Li-Carbon intercalation • Thermal stability of SEI • Reactivity of electrolyte

Mechanisms for Lithium Insertion in Carbonaceous Materials

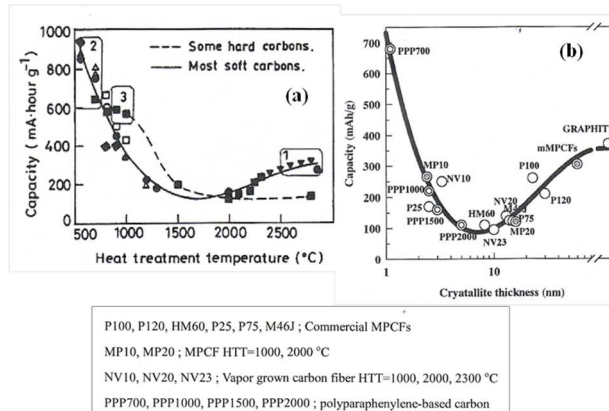


Figure 1-5. (a) Plot of reversible capacity for Li vs. HTT for a variety of carbon samples (□ hard carbon, ■ soft carbon), (b) Charge capacity as a function of the height of stacking (Lc002)

J. R. Dahn,* Tao Zheng, Yinghu Liu, J. S. Xue SCIENCE, 270, 27 OCTOBER 1995

Characteristics of various materials

	Precursor	Advantages	Disadvantages
Graphite (over 2800°C)	Natural graphite Artificial graphite MCMB Needle cokes VGCF	Low discharge potential (around 0.2V) Long cycle life	Low discharge capacity (372 mAh/g) High cost
Graphitizable carbon (600~800°C)	MCMB Meso phase pitch Green cokes	High capacity (700-1000mAh/g) Low cost	High discharge potential (around 1.0V) High irreversible capacity Poor cycle stability
Non-graphitizable carbon (1000~1400°C)	Thermosetting polymer Glassy carbon Coal Organic material Stabilized isotropic pitch	High capacity (400-700mAh/g) Low discharge potential (around 0.1V) Low cost	High irreversible capacity

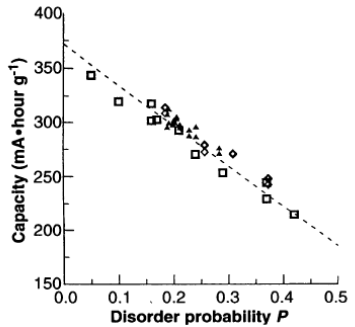


Fig. 3. Reversible capacity of region 1 carbons plotted as a function of the probability P of turbostratic disorder between adjacent carbon sheets. The line is the relation $Q = 372(1 - P)$, where Q is the capacity. For the purposes of this plot, samples corresponding to different symbols are equivalent.

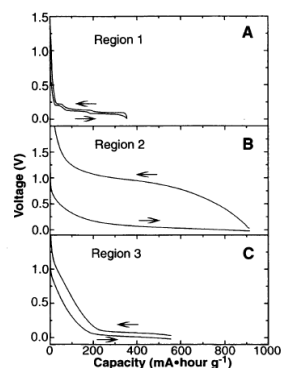
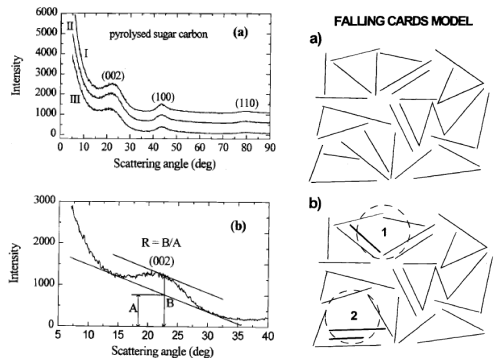
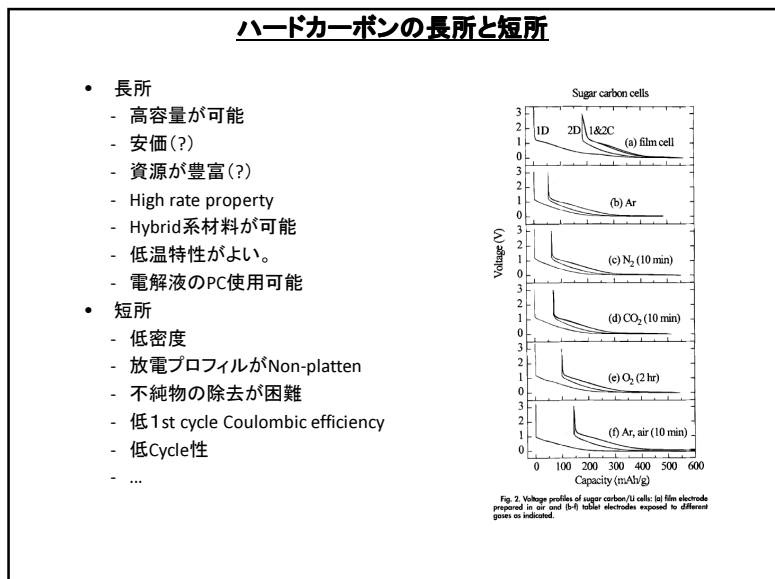
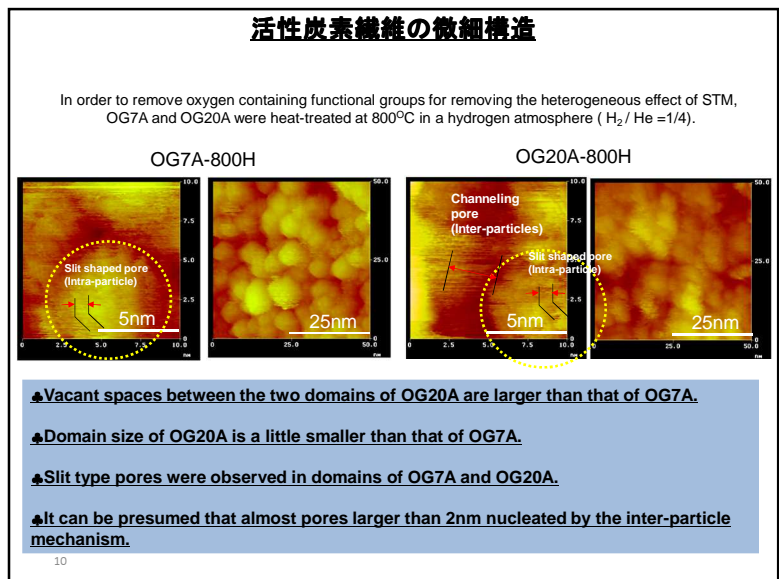
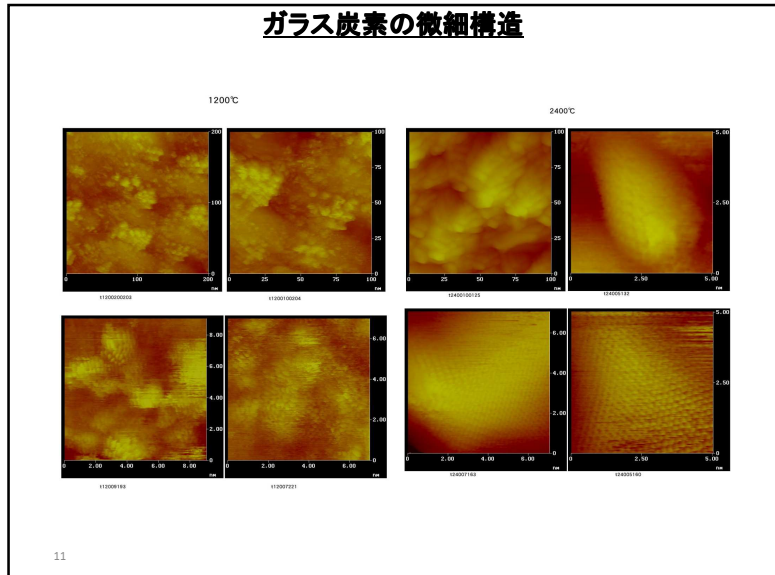
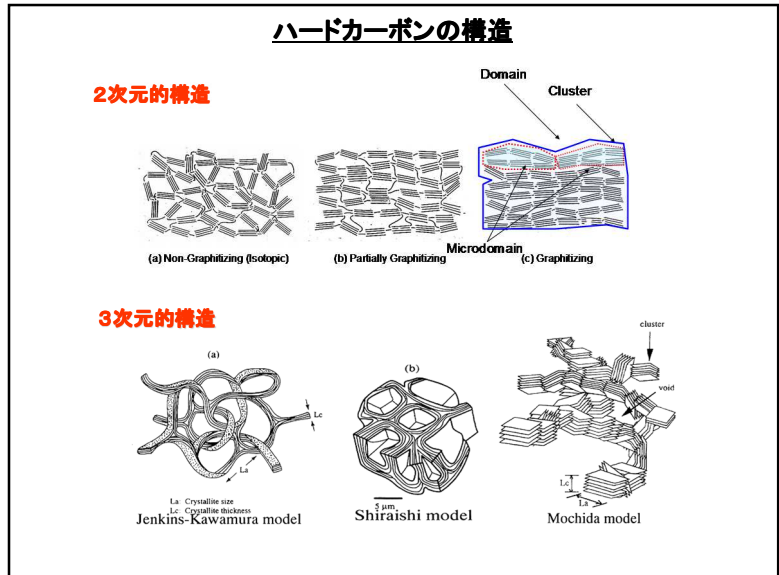


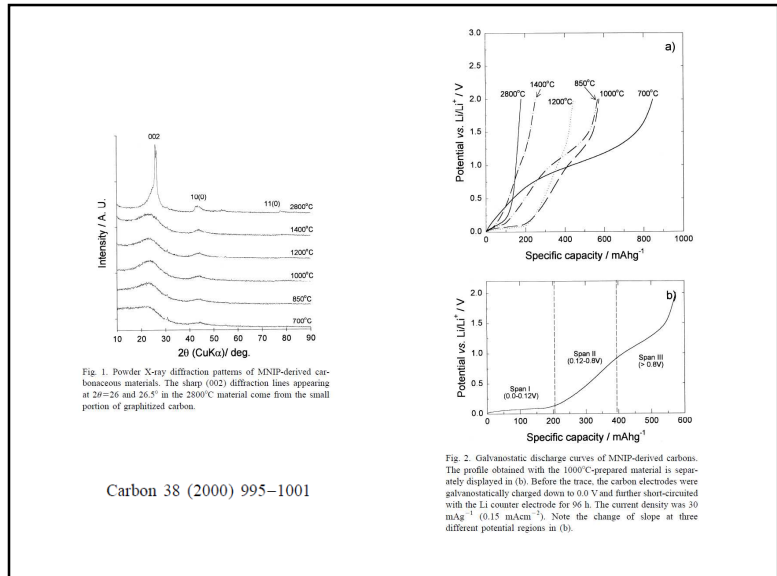
Fig. 2. Plots of voltage versus reversible capacity for the second charge-discharge cycle of representative carbon samples from regions 1, 2, and 3 of Fig. 1. (A) Synthetic graphite (Johnson-Matthey); (B) petroleum pitch (Crowley Tar Co.) heated to 550°C; (C) resole resin (Occidental Chemical Co.) heated to 1000°C. Arrows designate the directions the curves are traversed as Li is added to (to the right) or removed from (to the left) the carbon samples.

ハードカーボンの製造

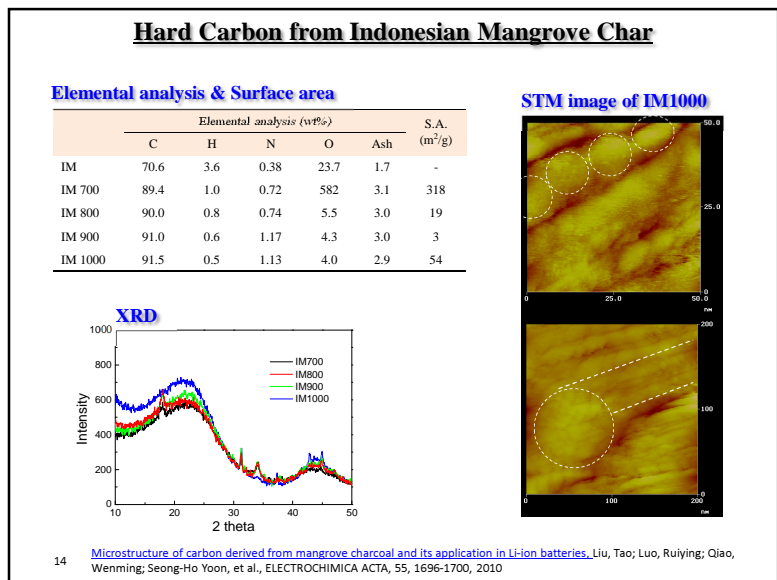
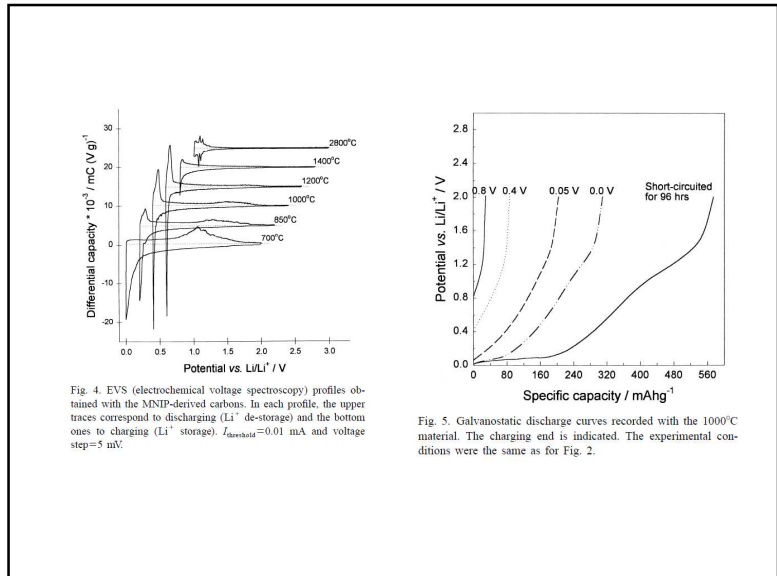
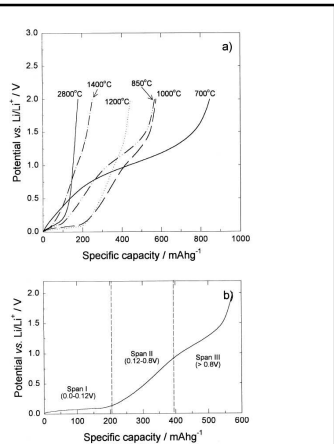
- 原料:難黒鉛化性前駆体
 - Biomass: Husk, Cellulose, Sugar, Rignin, Tree, Crab (Chichin), ...
 - Polymer: Phenol Resin, Unsaturated Resin, Epoxy Resin
 - Pitch: Isotropic Pitch and Coke
- 热处理温度
 - 800~1400°C
- 構造
 - 難黒鉛化性カーボン



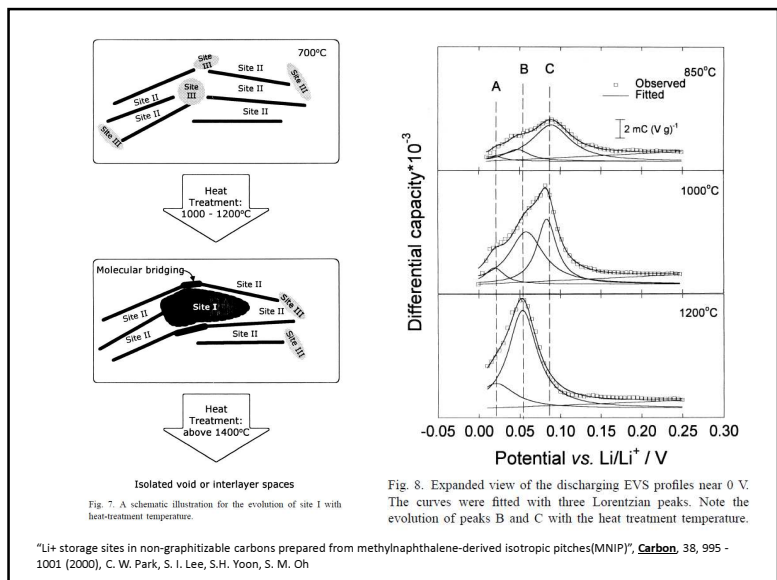




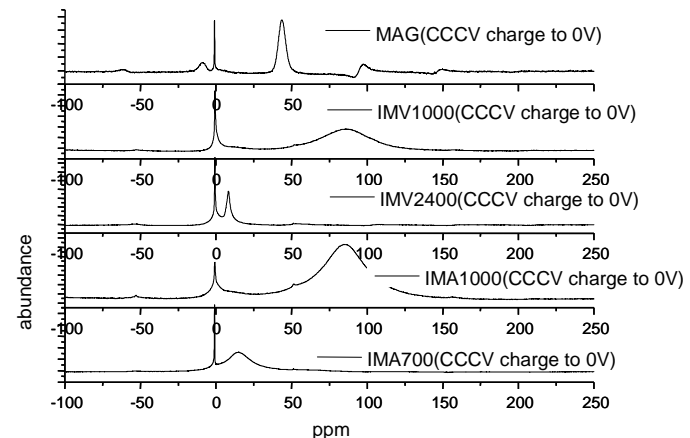
Carbon 38 (2000) 995–1001



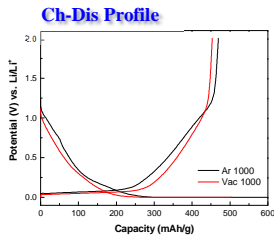
14 Microstructure of carbon derived from mangrove charcoal and its application in Li-ion batteries, Liu, Tao; Luo, Ruiying; Qiao, Wenming; Seong-Ho Yoon, et al., ELECTROCHIMICA ACTA, 55, 1696-1700, 2010



Li-NMR of Various Carbons



Hard Carbon from Indonesian Mangrove Char

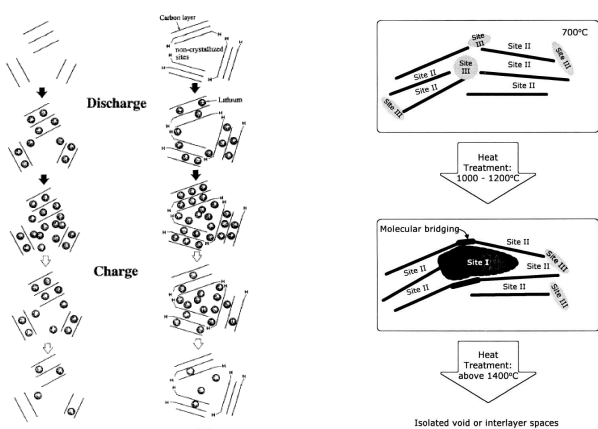


	Condition	Ch (mAh/g)	Dis (mAh/g)	Efficiency (1cy, %)	Cap _{ave} (mAh/g)
IM	Ar 1000	628	469	74.7	159
	Vac 1000	503	453	90.1	50

IM V1000 showed the better initial efficiency than that of IM Ar1000

19

ハードカーボンの充放電機構



Low-crystallized carbon materials for lithium-ion secondary batteries,
Hayato Higuchi, Keiichiro Uenae, Akira Kawakami
JOURNAL OF POWER SOURCES, 68, 1997

理想的なハードカーボン

- 高密度: 1.9g/cm³以上
- 高容量: 650mAh/cc
- 高レート性: 90%以上 (5C/0.2C: Half cell, 20C/0.2C:Single cell)
- Low Impurity: 100ppm以下
- 安価: 800円/Kg以下
- 高1st Coumbic efficiency
- 高低温特性
- 高サイクル性
- 豊富な原料からの調製
- マイルドな炭化条件
- Hybrid系が可能な材料: SnO_xまたはSiとのハイブリッド化⇒高容量化

⇒ 達成するためには、各々因子に対応する原因把握が要求。

⇒ まだ、原因解明が明らかになっていない。

⇒ 今後の研究に期待する。

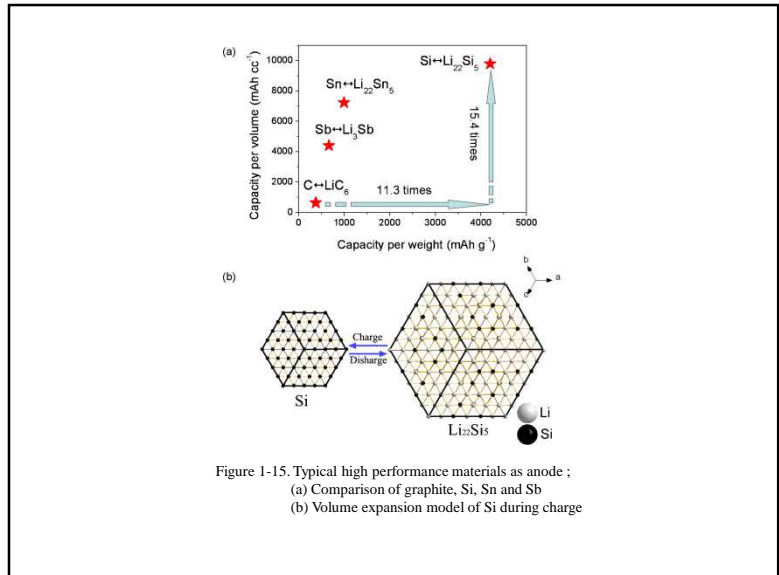


Figure 1-15. Typical high performance materials as anode;
(a) Comparison of graphite, Si, Sn and Sb
(b) Volume expansion model of Si during charge

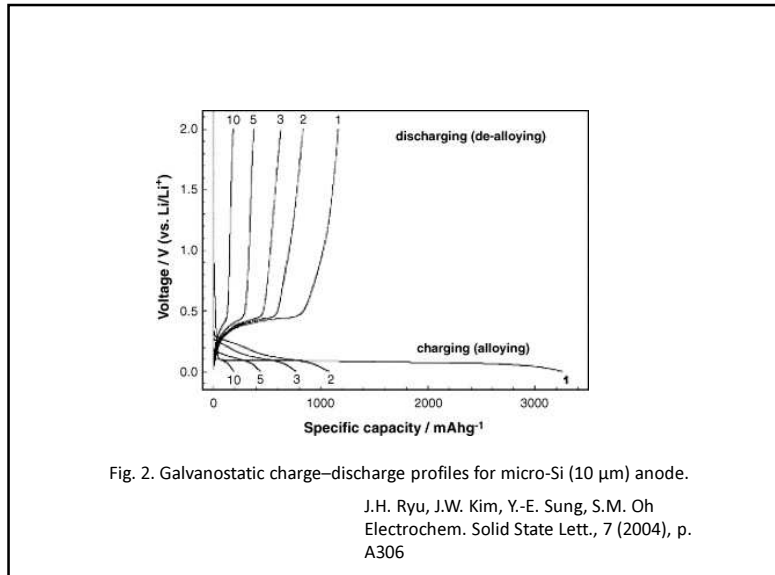
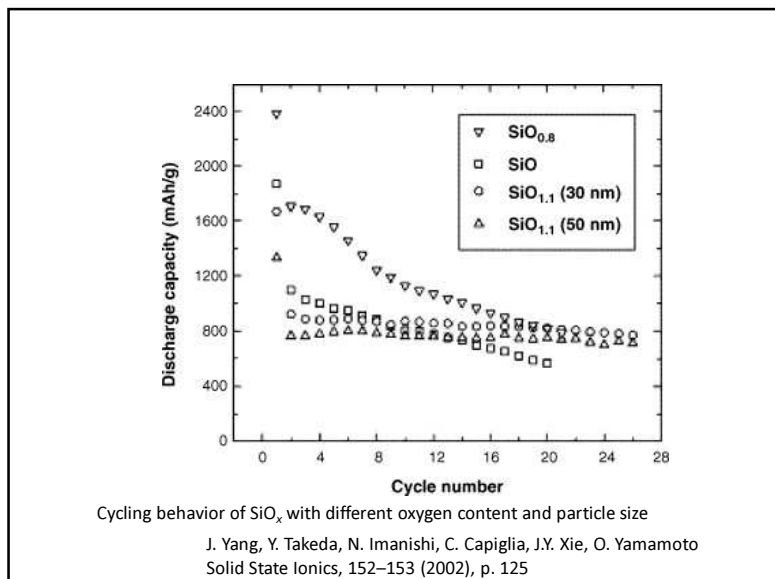
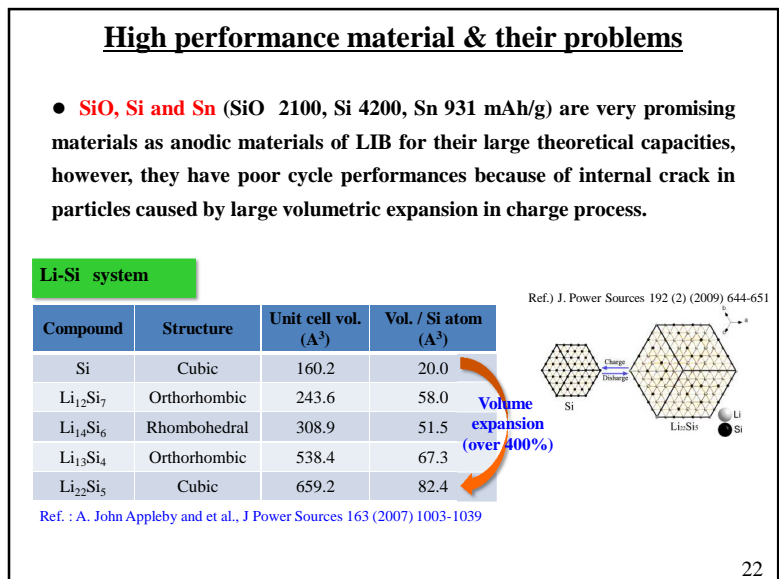
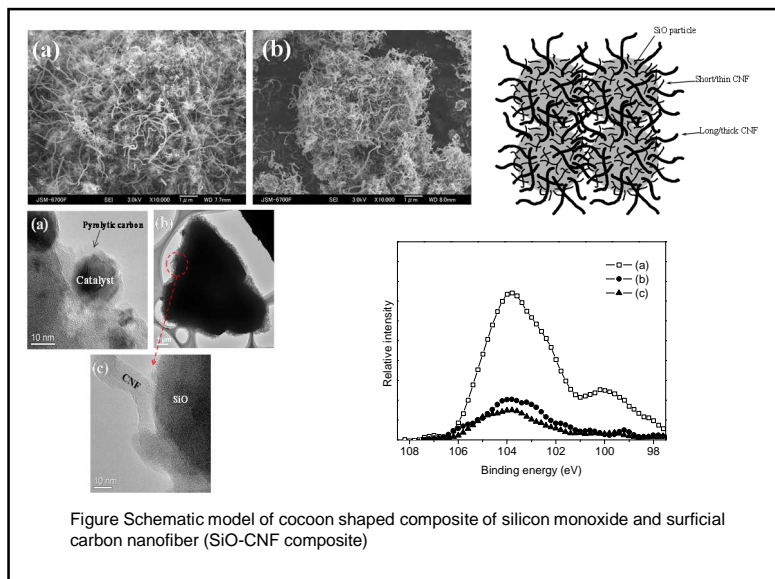
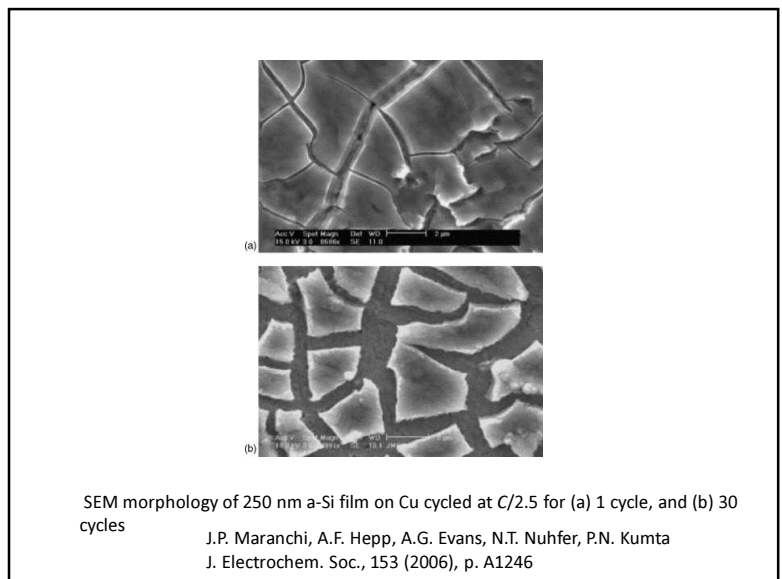
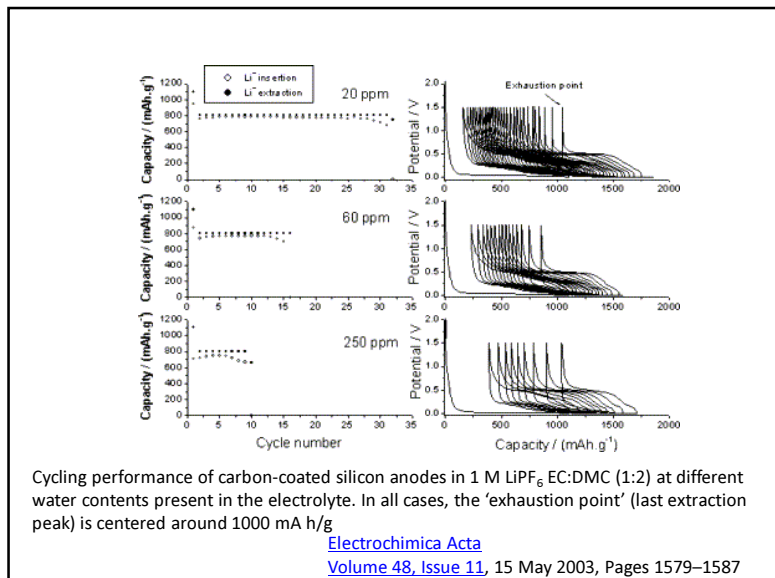
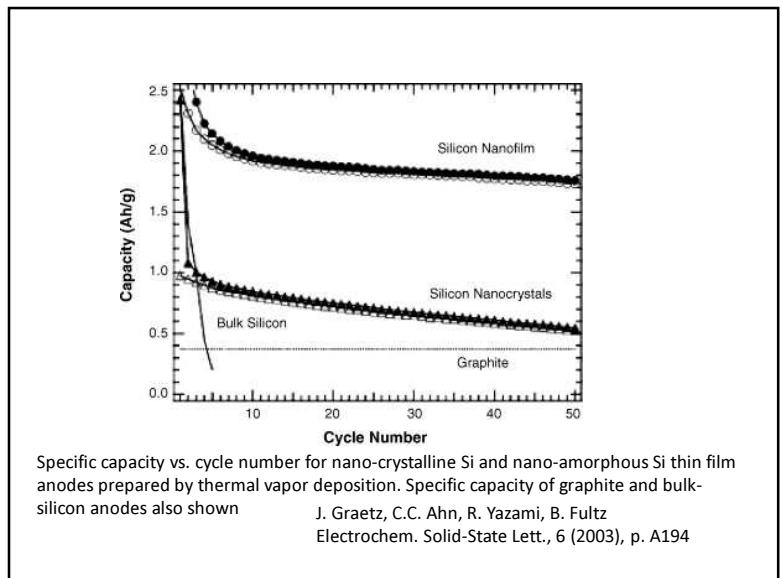


Fig. 2. Galvanostatic charge–discharge profiles for micro-Si (10 μm) anode.
J.H. Ryu, J.W. Kim, Y.-E. Sung, S.M. Oh
Electrochim. Solid State Lett., 7 (2004), p. A306





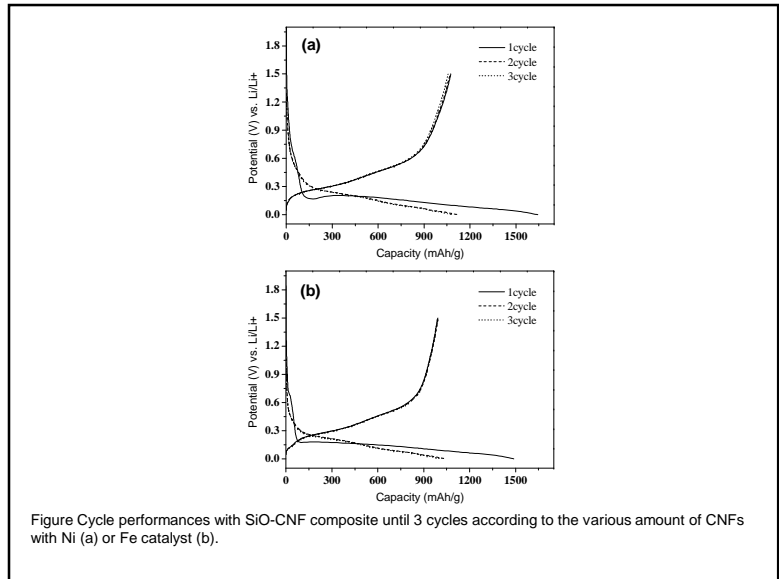


Figure 2-11: Cycle performances with SiO-CNF composite until 3 cycles according to the various amount of CNFs with Ni (a) or Fe catalyst (b).

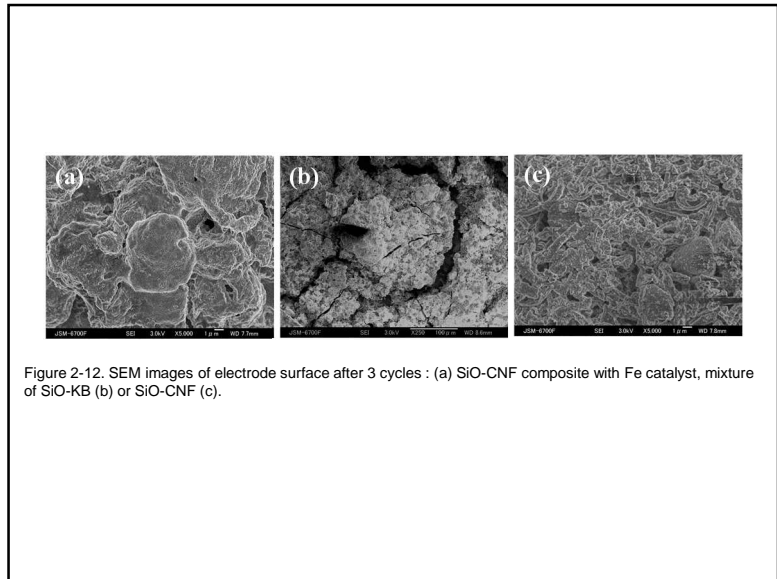
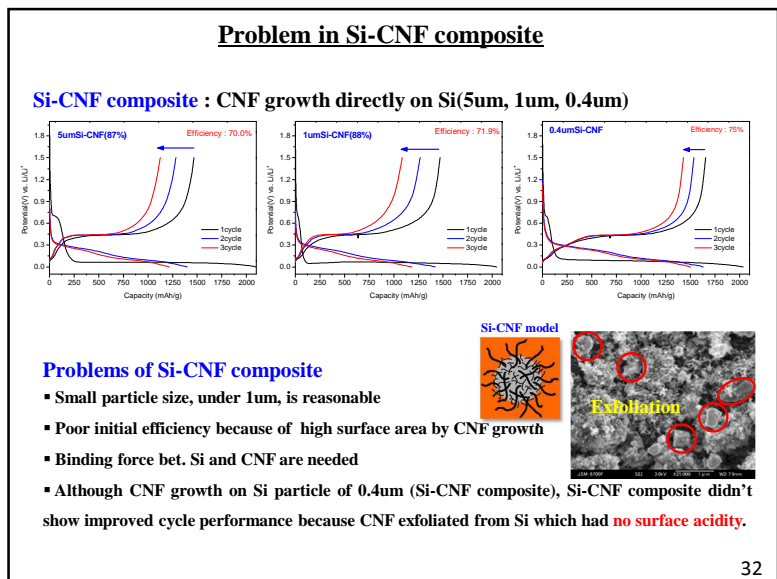
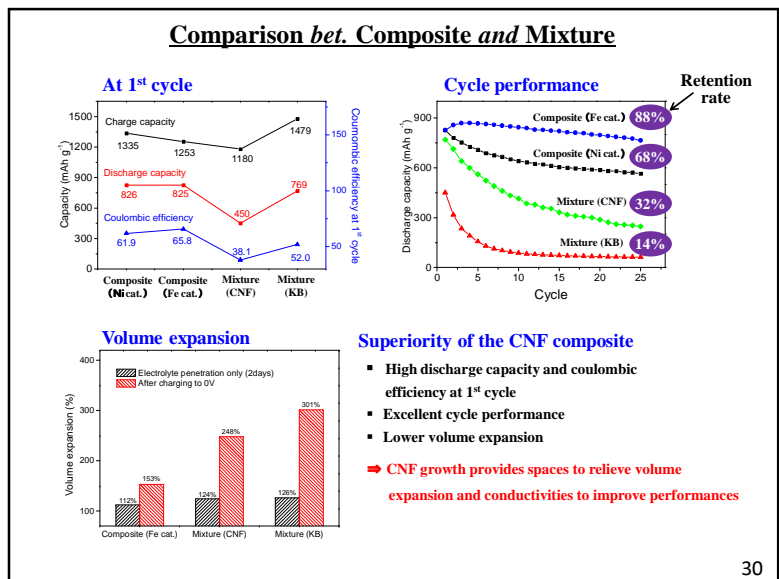
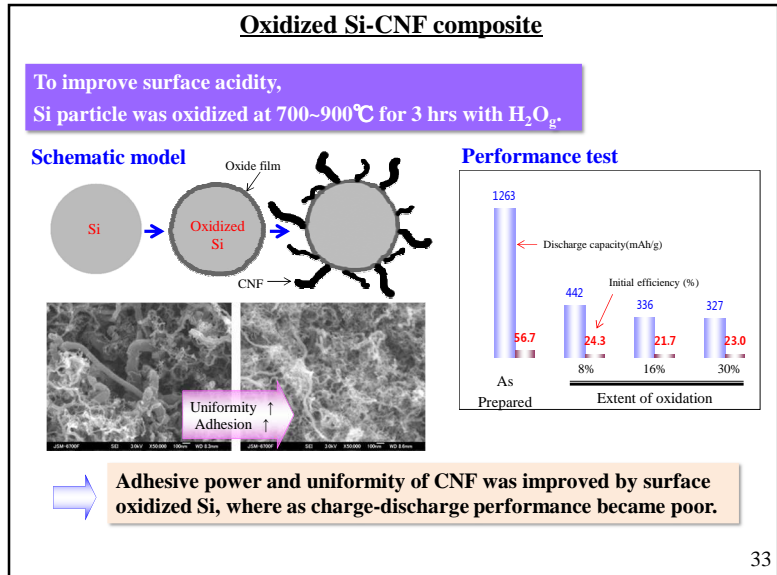


Figure 2-12: SEM images of electrode surface after 3 cycles : (a) SiO-CNF composite with Fe catalyst, mixture of SiO-KB (b) or SiO-CNF (c).



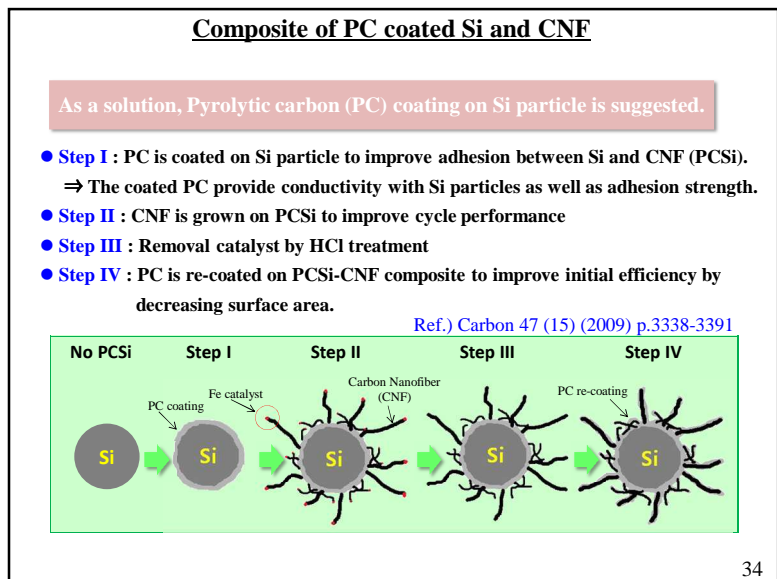


33

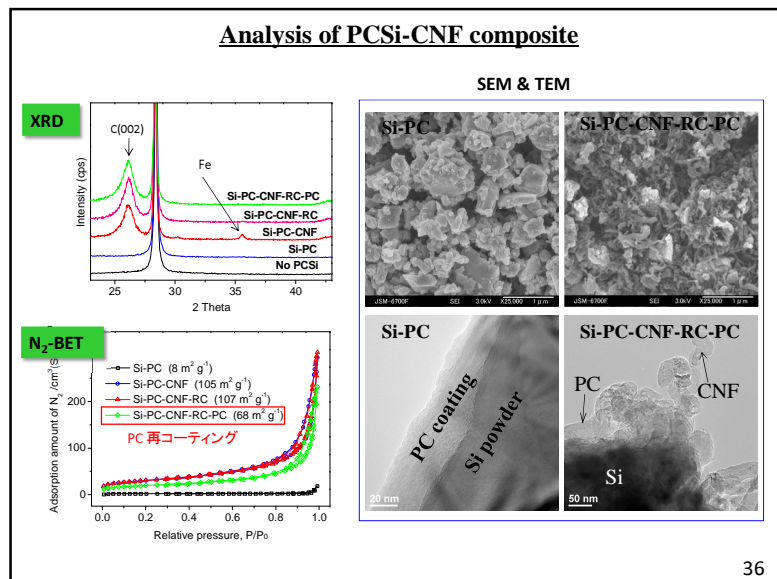
Preparation of PCSi-CNF composite

Samples	Code	PC/ or CNF amount (wt. %)			Condition
		PC	CNF	PC re-coating	
Step I	Si-PC	6 %	-	-	PC coating (900°C-CH ₄ /He- 30min)
Step II	Si-PC-CNF	6 %	93 %	-	CNF growth on PCSi (580°C-CO/He- 30min)
Step III	Si-PC-CNF-RC	6 %	93 %	-	Catalyst removal by HCl
Step IV	Si-PC-CNF-RC-PC	6 %	93 %	8 %	PC re-coating (900°C-CH ₄ /He- 30min)
Comparison	Si-CNF	-	98 %	-	CNF growth directly on Si surface

35

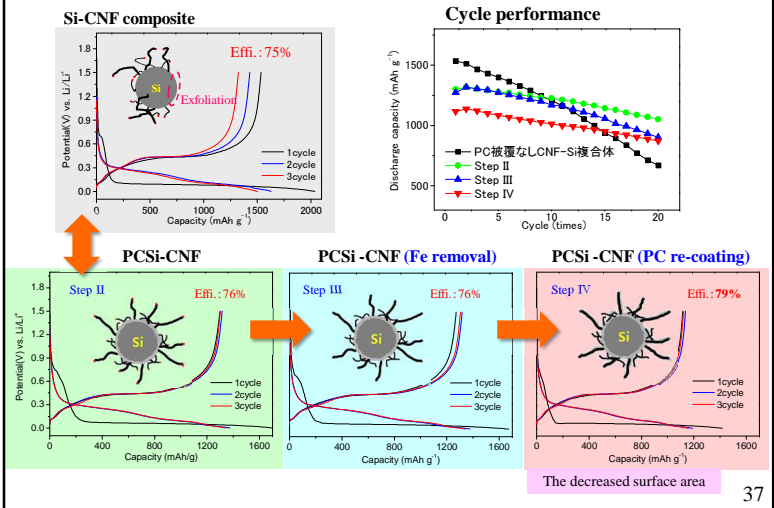


34



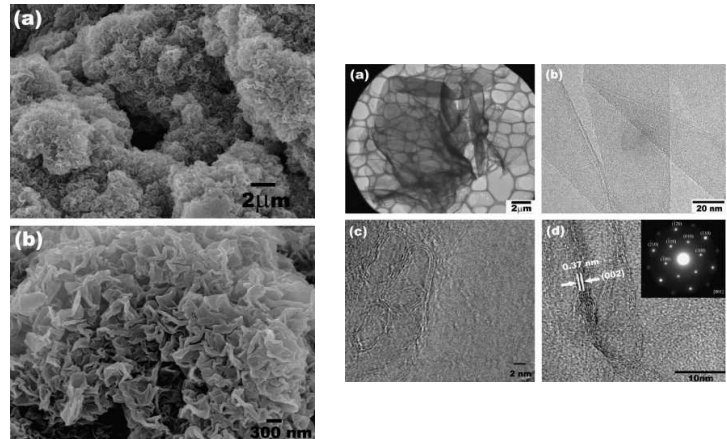
36

Cycle performances of PCSi-CNF composite



Graphene nanosheets for enhanced lithium storage in lithium ion batteries

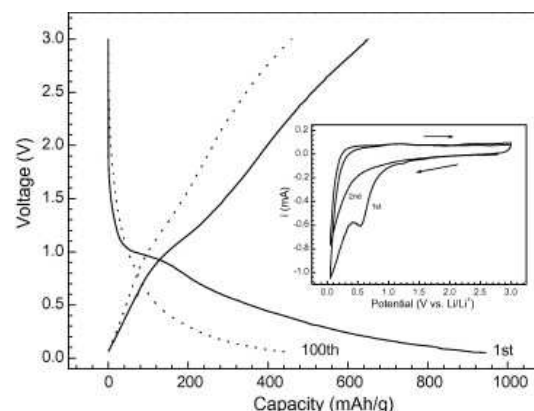
[Carbon, 47, 2009, 2049–2053, G. Wang et al.](#)



Cycle performances of PCSi-CNF composite

	Capacity at 1 st cycle (mAh/g)		
	Ch	Dis	效率(%)
Si-PC-CNF	1709	1299	76.0
Samples	Si-PC-CNF-RC	1674	1272
Comparison	Si-CNF	2037	1535
	78.8		75.4
	Dis.(max) (mAh/g)	At 20 cycle (mAh/g)	
		Dis	Retention rate (%)
Si-PC-CNF	1317	1051	80
Samples	Si-PC-CNF-RC	1318	903
Comparison	Si-CNF	1535	670
	77		44

38

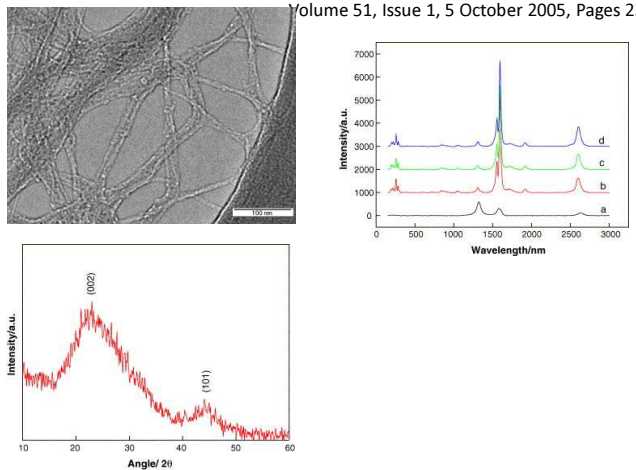


Charge and discharge curves of graphene nanosheets as anode in lithium-ion cells. The inset is the cyclic voltammograms of graphene nanosheet electrode

Single wall carbon nanotube paper as anode for lithium-ion battery

Electrochimica Acta

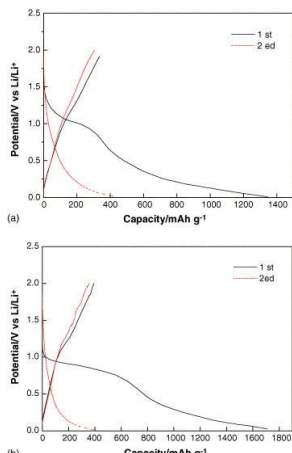
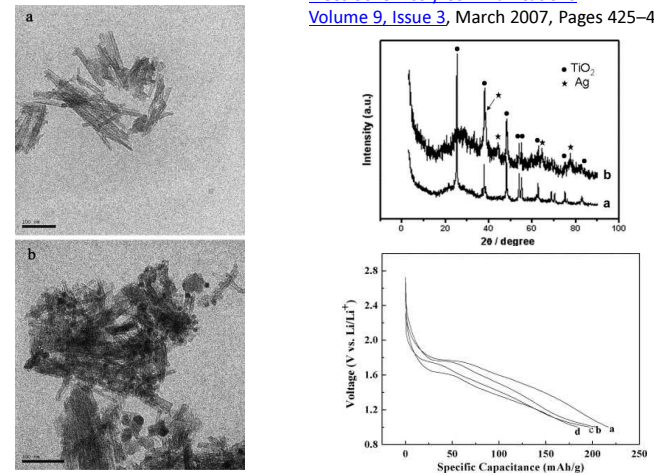
Volume 51, Issue 1, 5 October 2005, Pages 23–28



Preparation and electrochemical properties of Ag-modified TiO₂ nanotube anode material for lithium-ion battery

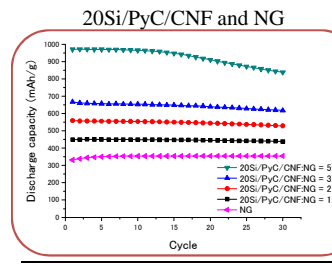
Electrochemistry Communications

Volume 9, Issue 3, March 2007, Pages 425–430

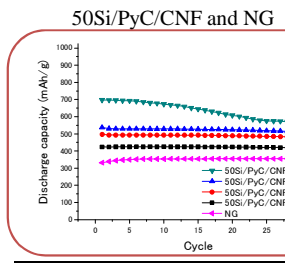


The charge/discharge profiles of SWNT electrodes: (a) conventional slurry coated electrode and (b) "Free standing" electrode.

Hybridization of Si/PyC/CNF and NG



Sample	1 st cycle Coulombic efficiency (%)	Retention ratio (% , 30 th /1 st)
20Si/PyC/CNF:NG=5:5	63.6	86.3
20Si/PyC/CNF:NG=3:7	67.5	92.6
20Si/PyC/CNF:NG=2:8	74.2	94.5
20Si/PyC/CNF:NG=1:9	80.3	97.7
NG	90.0	106.9



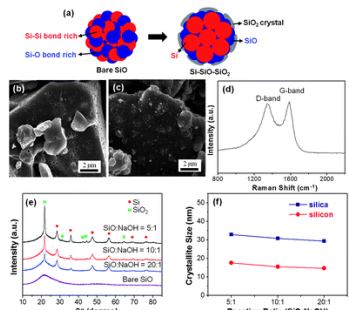
Sample	1 st cycle Coulombic efficiency (%)	Retention ratio (% , 30 th /1 st)
50Si/PyC/CNF:NG=5:5	63.1	81.4
50Si/PyC/CNF:NG=3:7	66.9	95.4
50Si/PyC/CNF:NG=2:8	72.1	96.7
50Si/PyC/CNF:NG=1:9	77.8	98.8
NG	90.0	106.9

✓ The hybrids of the Si/PyC/CNF and NG showed better cycle-ability than the hybrids of Si/PyC and NG.

Highly stable Si-based multicomponent anodes for practical use in lithium-ion batteries

Jung-In Lee , Nam-Soon Choi and Soojin Park
Energy Environ. Sci., 2012, 5, 7878-7882

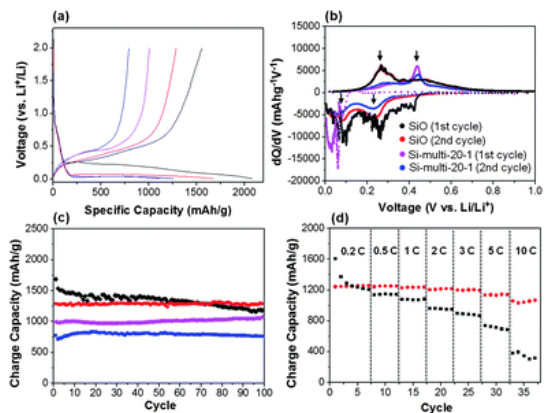
Interdisciplinary School of Green Energy, Ulsan National Institute of Science and Technology, Ulsan, Korea 689-798



Synthesis of an Si-based multicomponent from bulk SiO particles via thermal annealing in the presence of NaOH. (a) Schematic illustration for the conversion of bare SiO to Si-SiO-SiO₂ three-components. (b) SEM image of Si-based multicomponents, SEM image (c) and Raman spectrum (d) of carbon-coated Si-based multicomponents, (e) XRD patterns of Si-based multicomponents as a function of NaOH amount, and (f) calculation of silica and silicon crystallite size as a function of NaOH amount

まとめ

- Bulk Carbon以外は、長所と共に短所も持っております、まだLi-ion電池用負極としては商品化されていない。
- 今後の研究によって短所が解決できれば、電池の特性はより改善できる。



Electrochemical performances of c-SiO and c-Si-SiO-SiO₂ three-component electrodes. (a) Voltage profiles of c-SiO (black), c-Si-multi-20-1 (red), c-Si-multi-10-1 (pink), and c-Si-multi-5-1 (blue). (b) dQ/dV plots of c-SiO and c-Si-multi-20-1 (red) in the first and second cycles. (c) Cycle performances of c-SiO (black), c-Si-multi-20-1 (red), c-Si-multi-10-1 (pink), and c-Si-multi-5-1 (blue) at 0.1 C rate. (d) Rate capabilities of c-SiO and c-Si-multi-20-1 electrodes. The discharge rate was fixed at a rate of 0.1 C